Journal of Solid State Chemistry **144,** 91–99 (1999)
Article ID jssc.1998.8123, available online at http://www.idealibrary.com on IDEAL®

Phase Relations in the System In_2O_3–TiO_2–Fe_2O_3 at 1100°C in Air

Francisco Brown, Maria J. R. Flores, and Noboru Kimizuka[1]

Centro de Investigaciones en Polimeros y Materiales, Universidad de Sonora, Hermosillo, Sonora, C.P. 83000, Mexico

Yuichi Michiue, Mitsuko Onoda, Takahiko Mohri, and Masaki Nakamura

National Institute for Research in Inorganic Materials, 1-1 Namiki, Tsukuba-shi, Ibaraki-ken 305-0044, Japan

and

Nobuo Ishizawa

Research Laboratory of Engineering Materials, Tokyo Institute of Technology, 4259 Nagatsuda, Midori-ku, Yokohama-shi, 227 Japan

Received July 14, 1998; in revised form November 15, 1998; accepted November 25, 1998

Phase relations in the system In_2O_3–TiO_2–Fe_2O_3 at 1100°C in air are determined by means of a classic quenching method. There exist In_2TiO_5, Fe_2TiO_5 having a pseudo-Brookite-type phase and a new phase, $In_3Ti_2FeO_{10}$ having a solid solution range from In_2O_3:TiO_2:Fe_2O_3 = 4:6:1 to In_2O_3:TiO_2:Fe_2O_3 = 0.384:0.464:0.152 (mole ratio) on the line "$InFeO_3$"–"$In_2Ti_2O_7$." The crystal structures of $In_3Ti_2FeO_{10}$ are pyrochlore related with a_m = 5.9171 (5) Å, b_m = 3.3696 (3) Å, c_m = 6.3885 (6) Å, and β = 108.02 (1)° in a monoclinic crystal system at 1100°C, and a_0 = 5.9089 (5) Å, b_0 = 3.3679 (3) Å, and c_0 = 12.130 (1) Å in an orthorhombic system at 1200°C. The relationship between the lattice constants of these phases and those of the cubic pyrochlore type are approximately as follows: $a_m = -\frac{1}{4}a_p + (-\frac{1}{2})b_p + (-\frac{1}{4})c_p$, $b_m = -\frac{1}{4}a_p + (0)b_p + (\frac{1}{4})c_p$, $c_m = \frac{1}{4}a_p + (-\frac{1}{2})b_p + (\frac{1}{4})c_p$ and β = 109.47° in the monoclinic system, and $a_0 = -\frac{1}{4}a_p + (-\frac{1}{2})b_p + (-\frac{1}{4})c_p$, $b_0 = -\frac{1}{4}a_p + (0)b_p + (\frac{1}{4})c_p$, and $c_0 = \frac{2}{3}a_p + (-\frac{2}{3})b_p + (\frac{2}{3})c_p$ in the orthorhombic system, where $a_p = b_p = c_p$ = 9.90 (Å) are the lattice constants of "$In_2Ti_2O_7$" having the cubic pyrochlore type. All solid solutions of $In_3Ti_2FeO_{10}$ have incommensurate structures with a periodicity of $q \times b^*$ (q = 0.281–0.356) along the b^* axis and the stoichiometric phase has $q = \frac{1}{3}$. $InFeO_3$ having a layered structure type is unstable between 750 and 1100°C. © 1999 Academic Press

INTRODUCTION

Some complex oxides that contain In(III) have interesting physical properties such as transparency in the visible range and high electrical conductivity at room temperature. In addition, In(III) in crystalline oxides has unique crystal–chemical properties. It is located between Lu(III) and Sc(III) in ionic radius and takes the coordination number of 4, 5, 6, or 8, whereas the coordination numbers of rare earth elements (La–Lu, Y, and Sc) are 6 or higher (1). In_2O_3 under normal pressure has the C-type R_2O_3 crystal structure (R = Ho,–Lu, Y, or Sc) and is transformed into the ilmenite-type structure under high pressure (2). R_2O_3 is well known to transform into the B-type structure under high pressure (3). After completing our study of phase relations in the system In_2O_3–ZnM_2O_4–ZnO at 1350°C (M = Fe, Ga, or Al) and the crystal structures of homologous compounds, $(ZnO)_mIn_2O_3$ and $(ZnO)_mInMO_3$ having layered structures and $(ZnO)_mGa_2O_3$ (m = natural number) (4–9), we started studying ternary systems that contain In_2O_3 and TiO_2 as components. In the system In_2O_3–TiO_2–MO (M = Zn or Mg) at 1350°C, $(ZnO)_mIn(Ti_{1/2}Zn_{1/2})O_3$ having layered structures or $(MgO)In(Ti_{1/2}Mg_{1/2})O_3$ having a spinel-type structure were synthesized (10). In this paper, we report the phase relations in the system In_2O_3–TiO_2–Fe_2O_3 in air at 1100°C and crystal structure data of a new phase, $In_3Ti_2FeO_{10}$ with a pyrochlore-related structure and a phase transformation between monoclinic (lower-temperature phase) and orthorhombic (higher-temperature phase), clarified by means of X-ray powder and electron diffractometry.

Compounds of the layered $(ZnO)_m(In_2O_3)_n$ type (m, n = natural number) do not exist in the present system.

EXPERIMENTAL

A classic quenching method was employed, using oxide powders as starting compounds.

[1]To whom correspondence should be addressed at A. Postal 792, Hermosillo, Sonora, C.P. 83000 Mexico. E-mail: nkimizuk@guaymas.uson.mx.

0022-4596/99 $30.00

Starting Compounds

Powders of In_2O_3 (99.9%), TiO_2 (99.9%), and Fe_2O_3 (99.9%) were used. Prior to mixing, the powders were heated in air at 850°C for 1 day. In_2O_3 had the C-type structure, TiO_2 the rutile- type structure, and Fe_2O_3 the ilmenite-type structure. The particle size of the starting compounds was on the order of micrometers.

Calculated weights of the starting compounds were weighed and mixed under ethanol in an agate mortar for about 25 min. About 40 mixtures were made and heated at 1100°C in air, and phase analyses for the specimens were performed to establish the phase relations in the present ternary system.

Facilities

A vertical electric furnace with a SiC heating element was used. Temperature fluctuation in the furnace was controlled within ± 1°C. We used a box-type of furnace with a Mo–Si alloy heating element for preparation of specimens above 1100°C.

An X-ray powder diffractometer (Rigaku D-Max) with Cu$K\alpha$ radiation with a graphite monochromator, an electron microscope (Hitachi 400), and a scanning electron microscope (JEOL JSM-T200) were used for phase analyses, and lattice constants of the specimens were determined by means of the least-squares method. Si powder (NBS, Standard Reference Material 640b, $a = 5.4309$ Å) was used as the standard for calibration of the lattice constant measurement.

Experimental Procedures

All mixtures in the ternary system were heated in Pt crucibles in air. The weight of each specimen was monitored before and after heating. Evaporation was negligible within experimental error. After the samples were heated for fixed periods, they were rapidly cooled at room temperature, and X-ray powder diffractometry was used to identify the phases and determine the lattice constants. Some specimens were supplied for SEM observation to confirm phase assemblage. After repeated cycles of heating and grinding of the specimens, we concluded that equilibrium was obtained when the X-ray diffraction patterns indicated no further changes. To index the X-ray powder diffraction peaks of a new phase in the ternary system, the powders were examined by electron diffractometry. Since reaction rates at $T = 1000$°C were too slow to reach equilibrium in a timely manner, $T = 1100$°C was chosen for this study. A detailed description of the experimental method is given in (4).

RESULTS AND DISCUSSION

Phase Relations in the System In_2O_3–TiO_2–Fe_2O_3 at 1100°C in Air

The phase relations in this system are shown in Fig. 1.

In_2O_3–TiO_2 system. Only one phase, In_2TiO_5, had been reported previously by Senegas *et al.* (11). It was synthesized at 1250°C for 24 h and the unit cell constants were $a = 7.237$ Å, $b = 3.429$ Å, and $c = 14.86$ Å, which are similar to those for In_2VO_5. $In_2Ti_2O_5$ formed rapidly from In_2O_3 and TiO_2 at 1100°C and single-phase samples were formed within 1 or 2 days. Roth (12) synthesized $R_2Ti_2O_7$ through solid-state reactions between R_2O_3 (R = Sm, Gd, Dy, Yb, or Y) and TiO_2 powders at 1425–1550°C for 0.5–1 h in air, and reported that $R_2Ti_2O_7$ has the pyrochlore-type structure. $In_2Ti_2O_7$ could not be obtained from a reaction between In_2O_3 and TiO_2 powders at 1550°C for 3 h. Brixner synthesized $R_2Ti_2O_7$ (R = Sm–Lu, Y, or Sc) at 1200–1350°C for 10–14 h in air and measured the lattice constants (see Fig. 2), resistivities, and dielectric constants (13). In the present study at 1000 and 1100°C, $In_2Ti_2O_7$ was also not formed; however, as we describe later, there existed a phase having a pyrochlore-related structure in the ternary system In_2O_3–TiO_2–Fe_2O_3 close to the chemical composition In_2O_3:TiO_2 = 1:2 (mole ratio). Hereafter, we define this phase as unison-X_1. The lattice constant of In_2O_3 in

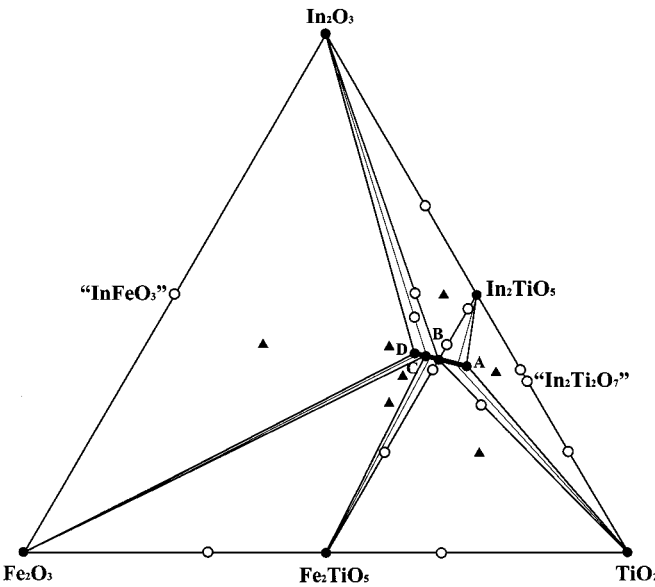

FIG. 1. Phase relations in the system In_2O_3–TiO_2–Fe_2O_3 at 1100°C in air: ●, a single phase exists; ○, two phases coexist; ▲, three phases coexist. Unison-X_1 phase has a solid solution range from point A (4:6:1) to point D (0.384:0.464:0.152) through points B (3:4:1) and C (0.380:0.480:0.140) along the line between "$InFeO_3$" and "$In_2Ti_2O_7$," where (u, v, w) represents the chemical composition ratio of In_2O_3:TiO_2:Fe_2O_3 (mole ratio). "$InFeO_3$" and "$In_2Ti_2O_7$" are unstable phases.

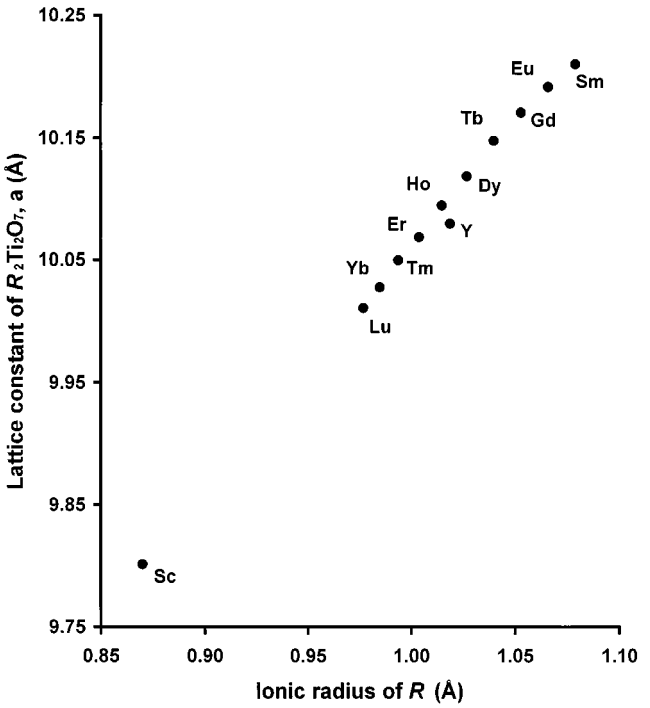

FIG. 2. Relationship between lattice constants of $R_2Ti_2O_7$ having cubic pyrochlore structure (13) and ionic radii of constituent R(III) with CN = 8 of oxygen cited from Ref. (1). R = Sm, Eu, Gd, Tb, Dy, Ho, Er, Tm, Yb, Lu, Y, or Sc.

equilibrium with In_2TiO_5 and the lattice constants of TiO_2 with In_2TiO_5 are listed in Tables 1A and 1B. We note that In_2O_3 in equilibrium with In_2TiO_5 has a smaller lattice constant than pure In_2O_3. We can safely conclude that In_2O_3 has a solid solution range toward In_2TiO_5 which is not explicitly shown in Fig. 1.

TiO_2–Fe_2O_3 system. There existed one phase Fe_2TiO_5 having the pseudo-Brookite-type structure with $a = 9.789$ (1) Å, $b = 9.973$ (2) Å, and $c = 3.7286$ (6) Å, which are identical within experimental error to $a = 9.7965$ (25) Å, $b = 9.9805$ (25) Å, and $c = 3.7301$ (1) Å for JCPDS Card No. 41-1432. Karkhanavala and Momin (14) reported the phase diagram for the system Fe_2O_3–TiO_2 at elevated temperatures in air in which there is only one phase, Fe_2TiO_5. Taylor established the phase diagram for the system TiO_2–FeO–Fe_2O_3 at 1300°C at various oxygen partial pressures, and also reported pseudo-Brookite Fe_2TiO_5 (15). These conclusions are consistent with the present study. The lattice constants of Fe_2O_3 in equilibrium with Fe_2TiO_5 and those of TiO_2 in equilibrium with Fe_2TiO_5 are listed in Table 1C.

TABLE 1B
Lattice Constants and Unit Cell Volumes of TiO_2 (Rutile Type), Space Group $P4_2/mnm$ (No. 136), in Equilibrium (a) Fe_2TiO_5 or (b) In_2TiO_5

	Fe_2TiO_5	In_2TiO_5	Starting compound	JCPDS (21-1276)
a (Å)	4.595 (1)	4.592 (1)	4.5927 (2)	4.5933
c (Å)	2.9511 (8)	2.9506 (7)	2.9582 (1)	2.9592
V (Å^3)	40.02	39.98	40.19	40.22

In_2O_3–Fe_2O_3 system. The present results indicate no binary compound in this subsystem. Shannon (2) reported $InFeO_3$ with an ilmenite-type structure with $a = 5.279$ Å and $c = 14.120$ Å, $V = 340.81$ Å^3, under $P = 65$ kbar at 1200°C. Nodari *et al.* (16) and Gerardin *et al.* (17) made $InFeO_3$ powders having a hexagonal layered structure with $a = 3.334$ Å and $c = 12.202$ Å, through coprecipitation of In $(OH)_3$ and Fe $(OH)_3$ in solution followed by heat treatment at 700°C in air, and reported that it decomposed at 800°C. Giaquinta *et al.* (18) made $InFeO_3$ single crystals from Bi_2O_3 flux at 1123 K for 3 days and reported single-crystal structural data. $InFeO_3$ is isostructural to the higher-pressure form of $InGaO_3$ (19).

We heated a mixture of In_2O_3:Fe_2O_3 = 1:1 at 750°C for 1 week and 1000°C for 4 + 7 + 7 days in a Pt crucible and obtained a mixture of In_2O_3 and Fe_2O_3 without forming $InFeO_3$. Also, a mixture of In_2O_3:Fe_2O_3:Bi_2O_3 = 1:1:1 (mole ratio) was heated at 750°C for 3 + 3 days and no $InFeO_3$ was obtained. Some ternary mixtures of In_2O_3, TiO_2, and Fe_2O_3 that were heated at 1000 and 1100°C also did not form the $InFeO_3$ phase. We conclude that layered

TABLE 1A
Lattice Constants and Unit Cell Volumes of In_2O_3, Space Group $I2_13$ (No. 199), in Equilibrium with (a) Fe_2O_3, (b) Fe_2O_3 and Unison-X_1,[a] or (c) In_2TiO_5

	Fe_2O_3	Fe_2O_3 + X_1	In_2TiO_5	Starting compound	JCPDS (6-416)
a (Å)	10.024 (2)	10.031 (1)	10.109 (3)	10.115 (1)	10.118
V (Å^3)	1007.2	1009.2	1033.3	1035.2	1035.8

[a]The starting mixture, In_2O_3:TiO_2:Fe_2O_3 = 4:4:2.

TABLE 1C
Lattice Constants and Unit Cell Volumes of Fe_2O_3, Space Group $R\bar{3}C$ (No. 167), in Equilibrium with (a) Fe_2TiO_5, (b) In_2O_3, or (c) In_2O_3 and Unison-X_1

	Fe_2TiO_5	In_2O_3	In_2O_3 + X_1	Starting compound	JCPDS (33-664)
a (Å)	5.0329 (1)	5.077 (1)	5.064 (3)	5.0345 (3)	5.0365 (1)
c (Å)	13.757 (2)	13.805 (3)	13.845 (8)	13.7468 (9)	13.7489 (7)
V (Å^3)	301.8	301.2	307.5	301.8	301.9

TABLE 2
The System In_2O_3–TiO_2–Fe_2O_3 at 1100°C in Air

No.	Mixing (mole) ratio of starting compounds, In_2O_3:TiO_2:Fe_2O_3	Heating period (days)	Phases obtained
01	1:0:1	4 + 7	In_2O_3, Fe_2O_3
02	0:3:7	4 + 7	Fe_2O_3, Fe_2TiO_5
03	0:7:3	4 + 7	Fe_2TiO_5, TiO_2
04	2:8:0	4 + 7	In_2TiO_5, TiO_2
05	35:65:0	4 + 7	TiO_2, In_2TiO_5
06	0:1:1	5 + 7	Fe_2TiO_5
07	1:1:0	7 + 7	In_2TiO_5
08	4:2:4	5 + 7 + 9	X_1, Fe_2O_3, In_2O_3
09	30:45:25	7 + 5	X_1, Fe_2O_3, Fe_2TiO_5
10	20:65:15	5 + 7	X_1, Fe_2TiO_5, TiO_2
11	4:6:1	5 + 7 + 9	X_1
12	2:5:3	4 + 7 + 5	X_1, Fe_2TiO_5
13	35:60:5	9 + 7 + 6	X_1, In_2TiO_5, TiO_2
14	50:45:5	9 + 7 + 6	In_2O_3, In_2TiO_5, X_1
15	65:35:0	9 + 7 + 6	In_2O_3, In_2TiO_5
16	4:5:1	7 + 6 + 5	X_1, In_2TiO_5
18	7:10:2	7 + 6 + 5	X_1
20	48:50:2	5 + 9 + 7	In_2TiO_5, X_1
22	3:4:1	9 + 7 + 7	X_1
23	35:45:20	9 + 7 + 7	X_1, Fe_2TiO_5, Fe_2O_3
24	3875:4500:1625	9 + 7 + 7	X_1, In_2O_3, Fe_2O_3
25	4:4:2	9 + 7 + 7	X_1, In_2O_3, Fe_2O_3
26	3:6:1	9 + 7 + 7	X_1, TiO_2
27	5:4:1	7 + 4 + 4	X_1, In_2O_3,
28	11:14:4	7 + 7 + 7	X_1
29	25:32:9	7 + 7 + 4	X_1
30	14:18:5	7 + 7 + 4	X_1
31	385:500:115	7 + 7 + 4	X_1, In_2TiO_5
32	36:50:14	7 + 7 + 4	X_1, Fe_2TiO_5
36	5:6:2	6 + 5 + 7	X_1, In_2O_3, Fe_2O_3
37	45:42:13	7 + 7	X_1, In_2O_3

$InFeO_3$ is unstable at 750–1100°C and that there exist no binary phases in the system In_2O_3–Fe_2O_3 at 1100°C. The lattice constants of In_2O_3 and Fe_2O_3, which are in equilibrium with each other, are listed in Tables 1A and 1C. We can see that the former are smaller than pure In_2O_3, and the latter are greater than pure Fe_2O_3. We conclude that In_2O_3 and Fe_2O_3 have a small solid solution range not explicitly shown in Fig. 1.

In_2O_3–TiO_2–Fe_2O_3 system. One phase was found, $In_3Ti_2FeO_{10}$ (In_2O_3:TiO_2:Fe_2O_3 = 3:4:1 or $InFeO_3$:$In_2Ti_2O_7$ = 1:1) near In_2O_3:TiO_2 = 1:2 (mole ratios). Unison-X_1 has a solid solution range on the line between "$InFeO_3$" and "$In_2Ti_2O_7$" from In_2O_3:TiO_2:Fe_2O_3 = 4:6:1 ($InFeO_3$:$In_2Ti_2O_7$ = 2:3) to 0.384:0.464:0.152 ($InFeO_3$:$In_2Ti_2O_7$ = 1.310:1.000). Unison-X_1 is brown. In the ternary system, there are five subareas in which three phases coexist: (1) In_2O_3, In_2TiO_5, and unison-X_1; (2) In_2O_3, Fe_2O_3, and unison-X_1; (3) unison-X_1, Fe_2O_3, and

TABLE 3A
X-Ray Powder Data of Unison-X_1 (In_2O_3:TiO_2:Fe_2O_3 = 3:4:1, Mole Ratio) in the System In_2O_3–TiO_2–Fe_2O_3 at 1100°C in Air[a]

h	k_1	l	k_2	$d_{obs.}$ (Å)	$d_{calc.}$ (Å)	I (%)
0	0	1	0	6.0685	6.0753	52
$\bar{1}$	1	1	$\bar{1}$	3.5388	3.5416	3
0	0	2	0	3.0351	3.0376	99
$\bar{2}$	0	1	0	2.9206	2.9206	9
$\bar{1}$	1	0	0	2.8893	2.8909	12
2	0	0	0	2.8113	2.8135	52
$\bar{1}$	1	1	0	2.7874	2.7879	100
2	0	0	1	2.7070	2.7105	4
$\bar{2}$	0	2	0	2.4817	2.4820	19
1	1	1	0	2.4607	2.4630	38
$\bar{2}$	0	2	1	2.4122	2.4104	1
2	0	1	0	2.2960	2.2965	12
$\bar{1}$	1	2	0	2.2815	2.2831	23
$\bar{1}$	1	1	1	2.2498	2.2521	3
1	1	1	1	2.0668	2.0701	2
$\bar{2}$	0	3	0	1.9552	1.9551	3
1	1	2	0	1.9433	1.9454	6
$\bar{3}$	1	1	$\bar{1}$	1.8363	1.8374	5
2	0	2	0	1.8050	1.8046	11
$\bar{1}$	1	3	0	1.7977	1.7983	31
2	0	2	1	1.7748	1.7765	1
$\bar{3}$	1	1	0	1.7018	1.7022	29
0	2	0	0	1.6851	1.6848	13
$\bar{3}$	1	2	0	1.6390	1.6393	10
3	1	0	0		1.6389	
0	2	1	0	1.6241	1.6235	4
$\bar{3}$	1	3	$\bar{1}$	1.5719	1.5725	4
3	1	1	$\bar{1}$		1.5718	
$\bar{3}$	1	1	1	1.5546	1.5549	4
$\bar{2}$	0	4	0	1.5527	1.5522	7
1	1	3	0	1.5470	1.5471	14
0	0	4	0	1.5185	1.5188	7
$\bar{3}$	1	3	0	1.4852	1.4852	19
3	1	1	0		1.4846	
$\bar{4}$	0	1	0	1.4733	1.4744	11
0	2	2	0		1.4733	
$\bar{4}$	0	2	0	1.4605	1.4603	5
$\bar{2}$	2	1	0		1.4594	
2	2	0	0	1.4459	1.4454	11
2	0	3	0		1.4453	
$\bar{1}$	1	4	0	1.4415	1.4422	8
4	0	0	0	1.4063	1.4068	1
$\bar{2}$	2	2	0	1.3941	1.3940	4
$\bar{3}$	1	3	1	1.3839	1.3843	2
3	1	1	1		1.3838	
$\bar{4}$	0	3	0	1.3707	1.3710	2
2	2	1	0	1.3585	1.3584	3
$\bar{3}$	1	4	0	1.3032	1.3033	1
3	1	2	0	1.3026	1.3027	1
$\bar{2}$	2	3	0	1.2760	1.2763	2
$\bar{2}$	0	5	0	1.2673	1.2672	1
1	1	4	0	1.2638	1.2644	3
$\bar{4}$	0	4	0	1.2411	1.2410	2
2	2	2	0	1.2319	1.2315	5
2	0	4	0	1.1911	1.1913	1
$\bar{1}$	1	5	0	1.1902	1.1897	2
4	0	2	0	1.1482	1.1483	1

TABLE 3A—*Continued*

h	k_1	l	k_2	$d_{obs.}$ (Å)	$d_{calc.}$ (Å)	I (%)
$\bar{2}$	2	4	0	1.1417	1.1415	5
$\bar{3}$	1	5	0	1.1332	1.1335	6
3	1	3	0		1.1330	
0	2	4	0	1.1279	1.1281	3
$\bar{5}$	1	2	0	1.1147	1.1145	2
$\bar{4}$	2	1	0	1.1090	1.1095	2
$\bar{5}$	1	1	0	1.1086	1.1082	2
$\bar{4}$	0	5	0	1.1039	1.1038	3
$\bar{4}$	2	2	0	1.1033	1.1035	3
1	3	0	0	1.1013	1.1015	2
2	2	3	0	1.0968	1.0970	2
$\bar{1}$	3	1	0	1.0958	1.0955	2
$\bar{5}$	1	3	0	1.0846	1.0846	1
4	2	0	0	1.0799	1.0798	1
1	3	1	0	1.0724	1.0725	2
5	1	0	0	1.0677	1.0674	1
$\bar{4}$	2	3	0	1.0635	1.0634	3
$\bar{2}$	0	6	0		1.0632	
$\bar{1}$	1	5	0	1.0614	1.0615	4
1	3	2	0	1.0560	1.0562	1
$\bar{5}$	1	4	0	1.0264	1.0264	1
$\bar{2}$	2	5	0	1.0127	1.0127	2
0	0	6	0		1.0125	

[a] k_2 is an index for the vector along the b^* axis with a periodicity of q $(= 0.333) \times b^*$. a, b, c, and β were calculated from d spacings of hk_1l0. d spacings of hk_1lk_2 were calculated from a, b, c, β, and $q = 0.333$.

Fe_2TiO_5; (4) unison-X_1, Fe_2TiO_5, and TiO_2; (5) unison-X_1,TiO_2, and In_2TiO_5. And there are five subareas in which the solid solution of unison-X_1 coexists with In_2O_3, In_2TiO_5, TiO_2, Fe_2TiO_5, or Fe_2O_3. The lattice constants of In_2O_3, Fe_2O_3, and unison-X_1, which are in equilibrium with each other, with a starting mixture of In_2O_3:TiO_2:Fe_2O_3 = 4:4:2, are listed in Tables 1A–1C and 4.

Starting mixtures, heating periods, and phases obtained in the present ternary system for establishing Fig. 1 are summarized in Table 2.

Crystal Structural Study of Unison-X_1

X-ray powder data of unison-X_1 (3:4:1) at 1100 and 1200°C are given in Tables 3A and 3B, and are very similar to those for $Lu_2Ti_2O_7$ having a cubic pyrochlore-type structure with $a = 10.011$ Å (JCPDS Card No. 23-0375). From electron diffractometry, we concluded that the lower-temperature form of $In_3Ti_2FeO_{10}$ is monoclinic and the higher-temperature form is orthorhombic, having a superlattice along the b^* axis with a periodicity of $\frac{1}{3} \times b^*$.

Figures 3A and 3B are photographs of the monoclinic phase and orthorhombic phase. Tables 3A and 3B give the results of four-dimensional indexing (hk_1lk_2) for each powder X-ray diffraction peak in Tables 3A and 3B, where k_1 is an index for b^* and k_2 is for $q \times b^*$ ($q = \frac{1}{3}$). The reason for

TABLE 3B
X-Ray Powder Data of Unison-X_1 (In_2O_3:TiO_2:Fe_2O_3 = 3:4:1, Mole Ratio) in the System In_2O_3–TiO_2–Fe_2O_3 at 1200°C in Air[a]

h	k_1	l	k_2	$d_{obs.}$ (Å)	$d_{calc.}$ (Å)	I (%)
0	0	2	0	6.0602	6.0649	55
1	1	1	$\bar{1}$	3.6591	3.6608	2
1	1	2	$\bar{1}$	3.2495	3.2443	2
0	0	4	0	3.0290	3.0325	100
2	0	0	0	2.9527	2.9545	18
1	1	0	0	2.9243	2.9260	31
2	0	1	0	2.8694	2.8705	9
1	1	1	0	2.8409	2.8444	18
1	1	3	$\bar{1}$	2.7874	2.7843	3
2	0	1	1	2.7606	2.7613	3
2	0	2	0	2.6555	2.6561	38
1	1	2	0	2.6343	2.6353	59
1	1	1	1	2.2804	2.2812	4
2	0	4	0	2.1165	2.1162	13
1	1	4	0	2.1043	2.1056	22
2	0	4	1	2.0749	2.0712	3
1	1	5	$\bar{1}$	2.0508	2.0509	3
2	0	5	0	1.8746	1.8749	1
1	1	5	0	1.8659	1.8676	3
3	1	0	$\bar{1}$	1.8335	1.8351	3
3	1	0	0	1.7001	1.7002	29
0	2	0	0	1.6839	1.6840	17
3	1	1	0		1.6838	
2	0	6	0	1.6692	1.6684	10
1	1	6	0	1.6631	1.6633	23
3	1	2	0	1.6380	1.6371	9
0	2	2	0	1.6226	1.6226	6
3	1	4	$\bar{1}$	1.5700	1.5700	4
3	1	3	0	1.5677	1.5673	2
3	1	0	1	1.5532	1.5527	2
0	0	8	0	1.5163	1.5162	8
1	1	7	0	1.4903	1.4910	2
3	1	4	0	1.4835	1.4830	20
0	2	4	0	1.4725	1.4722	12
2	2	0	0	1.4633	1.4630	2
2	2	1	0	1.4519	1.4525	2
4	0	2	0	1.4355	1.4353	4
2	2	2	0	1.4227	1.4222	8
3	1	5	0	1.3919	1.3923	1
3	1	4	1	1.3821	1.3824	2
2	0	8	0	1.3493	1.3490	2
1	1	8	0	1.3463	1.3462	4
4	0	4	0	1.3277	1.3280	3
2	2	4	0	1.3177	1.3177	3
3	1	6	0	1.3005	1.3012	2
2	2	5	0	1.2533	1.2528	1
4	0	6	0	1.1929	1.1927	1
2	2	6	0	1.1851	1.1852	4
3	1	8	0	1.1318	1.1316	8
0	2	8	0	1.1269	1.1268	5
4	0	7	0	1.1238	1.1242	4
1	1	10	0	1.1202	1.1205	3
2	2	7	0	1.1178	1.1179	2
5	1	0	0	1.1153	1.1151	4
4	2	0	0	1.1111	1.1105	3
5	1	1	0	1.1102	1.1104	3
1	3	0	0	1.1031	1.1029	2
1	3	1	0	1.0982	1.0984	2

TABLE 3B—*Continued*

h	k_1	l	k_2	$d_{obs.}$ (Å)	$d_{calc.}$ (Å)	I (%)
5	1	2	0	1.0970	1.0967	3
4	2	2	0	1.0924	1.0923	2
1	3	2	0	1.0852	1.0851	4
4	0	8	0	1.0584	1.0581	1
2	2	8	0	1.0532	1.0528	3
5	1	4	0	1.0466	1.0466	2
4	2	4	0	1.0426	1.0428	2
1	3	4	0	1.0362	1.0365	2
2	0	11	0	1.0329	1.0331	1
1	1	11	0	1.0320	1.0319	1
5	1	5	0	1.0128	1.0132	1
0	0	12	0	1.0110	1.0108	3

[a] k_2 is an index for the vector along the b^* axis with a periodicity of q $(= 0.333) \times b^*$. a, b, and c were calculated from d spacings of hk_1l0. d spacings of hk_1lk_2 were calculated from a, b, c, and $q = 0.333$.

not using normal three-dimensional unit cell constants having $3b$ is given later. Unison-X_1 with an "$In_2Ti_2O_7$"-rich composition in the solid solution range has a monoclinic system and that with an $InFeO_3$-rich composition has an orthorhombic system at 1100°C. We observed incommensurate diffraction spots with a spacing equal to q $(= 0.281–0.357) \times b^*$ along the b^* axis on electron diffraction photographs which also appeared as corresponding

TABLE 3C
X-Ray Powder Data of Unison-X_1 (In_2O_3:TiO_2:Fe_2O_3 = 4:6:1, Mole Ratio) in the System In_2O_3–TiO_2–Fe_2O_3 at 1100°C in Air[a]

h	k_1	l	k_2	$d_{obs.}$ (Å)	$d_{calc.}$ (Å)	I (%)
0	0	1	0	6.0520	6.0638	41
$\bar{1}$	1	1	$\bar{1}$	3.5951	3.6053	2
0	0	2	0	3.0290	3.0319	87
1	1	1	$\bar{1}$	2.9622	2.9716	3
$\bar{2}$	0	1	0	2.9169	2.9198	9
$\bar{1}$	1	0	0	2.8929	2.8976	12
2	0	0	0	2.8113	2.8125	52
$\bar{1}$	1	1	0	2.7908	2.7935	100
2	0	0	1	2.6959	2.6967	4
$\bar{2}$	0	2	0	2.4804	2.4802	16
1	1	1	0	2.4633	2.4659	38
2	0	1	0	2.2938	2.2946	12
$\bar{1}$	1	2	0	2.2837	2.2847	25
$\bar{1}$	1	1	1	2.2284	2.2276	2
1	1	1	1	2.0508	2.0505	2
$\bar{2}$	0	3	0	1.9528	1.9528	3
1	1	2	0	1.9449	1.9455	7
$\bar{3}$	1	1	$\bar{1}$	1.8425	1.8460	3
2	0	2	0	1.8016	1.8023	15
$\bar{1}$	1	3	0	1.7977	1.7978	31
2	0	2	1	1.7678	1.7707	1
$\bar{3}$	1	1	0	1.7030	1.7033	32
0	2	0	0	1.6879	1.6903	9
$\bar{3}$	1	2	0	1.6396	1.6401	9
3	1	0	0		1.6397	
0	2	1	0	1.6284	1.6282	4
$\bar{3}$	1	3	$\bar{1}$	1.5759	1.5771	3
3	1	1	$\bar{1}$		1.5764	
$\bar{2}$	0	4	0	1.5503	1.5499	6
1	1	3	0	1.5461	1.5461	13
0	0	4	0	1.5158	1.5160	7
$\bar{3}$	1	3	0	1.4852	1.4853	19
3	1	1	0		1.4848	
0	2	2	0	1.4763	1.4764	11
$\bar{4}$	0	1	0	1.4737	1.4740	5
$\bar{2}$	2	1	0	1.4625	1.4629	2
$\bar{4}$	0	2	0	1.4596	1.4599	4
2	2	0	0	1.4487	1.4488	9
2	0	3	0	1.4443	1.4432	5
$\bar{1}$	1	4	0	1.4407	1.4410	3
1	1	3	1	1.4258	1.4261	1
4	0	0	0	1.4059	1.4063	2
$\bar{2}$	2	2	0	1.3970	1.3968	5
$\bar{4}$	0	3	0	1.3703	1.3703	2
2	2	1	0	1.3602	1.3609	3
$\bar{3}$	1	4	0	1.3026	1.3028	1
3	1	2	0		1.3022	
$\bar{2}$	2	3	0	1.2781	1.2780	2
$\bar{2}$	0	5	0	1.2650	1.2652	2
1	1	4	0	1.2630	1.2630	2
$\bar{4}$	0	4	0	1.2406	1.2401	2
2	2	2	0	1.2330	1.2329	4
2	0	4	0	1.1889	1.1894	3
$\bar{1}$	1	5	0		1.1883	
4	0	2	0	1.1474	1.1473	2
$\bar{2}$	2	4	0	1.1425	1.1424	4
$\bar{3}$	1	5	0	1.1326	1.1327	4
3	1	3	0		1.1322	
0	2	4	0	1.1290	1.1286	5
$\bar{5}$	1	2	0	1.1147	1.1147	1
$\bar{4}$	2	1	0	1.1106	1.1109	1
$\bar{5}$	1	1	0	1.1082	1.1084	3
$\bar{4}$	2	2	0	1.1053	1.1049	3
1	3	0	0		1.1049	
$\bar{4}$	0	5	0	1.1023	1.1027	3
$\bar{1}$	3	1	0	1.0990	1.0989	4
2	2	3	0	1.0976	1.0976	2
$\bar{5}$	1	3	0	1.0848	1.0846	2
4	2	0	0	1.0811	1.0810	2
1	3	1	0	1.0753	1.0755	2
5	1	0	0	1.0676	1.0674	1
$\bar{4}$	2	3	0	1.0645	1.0645	3
$\bar{2}$	0	6	0	1.0615	1.0614	3
1	1	5	0	1.0596	1.0601	3
$\bar{1}$	3	2	0	1.0593	1.0591	2
$\bar{5}$	1	4	0	1.0261	1.0262	1
$\bar{2}$	2	5	0	1.0130	1.0129	1
0	0	6	0	1.0107	1.0107	2

[a] k_2 is an index for the vector along the b^* axis with a periodicity of q $(= 0.356) \times b^*$. a, b, c, and β were calculated from d spacings of hk_1l0. d spacings of hk_1lk_2 were calculated from a, b, c, β, and $q = 0.356$.

TABLE 3D
X-Ray Powder Data of Unison-X_1 (In_2O_3:TiO_2:Fe_2O_3 = 15:16:7 in a mole ratio) in the System In_2O_3–TiO_2–Fe_2O_3 at 1200°C in Air

h	k_1	l	k_2	$d_{obs.}$ (Å)	$d_{calc.}$ (Å)	I (%)
0	0	2	0	6.0685	6.0773	45
1	1	0	$\bar{1}$	3.7131	3.6683	2
1	1	1	$\bar{1}$	3.5005	3.5118	2
1	1	2	$\bar{1}$	3.1329	3.1415	2
0	0	4	0	3.0351	3.0387	100
2	0	0	0	2.9469	2.9489	20
1	1	0	0	2.9225	2.9249	35
2	0	1	0	2.8640	2.8658	14
1	1	1	0	2.8409	2.8437	26
2	0	1	1	2.7889	2.7873	2
1	1	3	$\bar{1}$	2.7228	2.7193	2
2	0	2	0	2.6525	2.6531	44
1	1	2	0	2.6328	2.6355	81
2	0	2	1	2.5884	2.5904	3
1	1	1	1	2.3548	2.3560	2
1	1	2	1	2.2325	2.2335	1
2	0	4	0	2.1165	2.1162	15
1	1	4	0	2.1062	2.1073	30
2	0	4	1	2.0820	2.0840	3
2	0	5	0	1.8746	1.8758	4
1	1	5	0	1.8688	1.8695	6
3	1	0	$\bar{1}$	1.8109	1.8128	4
3	1	0	0	1.6977	1.6979	27
0	2	0	0	1.6839	1.6841	14
3	1	1	0	1.6805	1.6816	9
2	0	6	0	1.6709	1.6698	10
1	1	6	0	1.6647	1.6653	28
3	1	2	0	1.6353	1.6353	7
0	2	2	0	1.6226	1.6230	3
3	1	0	1	1.5748	1.5745	3
3	1	4	$\bar{1}$	1.5564	1.5568	3
0	0	8	0	1.5194	1.5193	9
2	0	7	0	1.4959	1.4963	2
1	1	7	0	1.4920	1.4931	3
3	1	4	0	1.4822	1.4822	19
0	2	4	0	1.4733	1.4730	13
2	2	0	0	1.4621	1.4624	4
2	2	1	0	1.4515	1.4520	4
4	0	2	0	1.4324	1.4329	4
2	2	2	0	1.4219	1.4219	11
3	1	5	0	1.3919	1.3920	1
2	2	3	0	1.3753	1.3756	1
2	0	8	0	1.3506	1.3506	2
1	1	8	0	1.3483	1.3483	6
4	0	4	0	1.3261	1.3265	4
2	2	4	0	1.3177	1.3178	4
3	1	6	0	1.3014	1.3013	1
0	2	6	0	1.2949	1.2950	1
4	0	5	0	1.2613	1.2607	1
2	2	5	0	1.2533	1.2531	2
0	0	10	0	1.2158	1.2155	1
3	1	7	0	1.2146	1.2140	1
4	0	6	0	1.1916	1.1921	3
2	2	6	0	1.1858	1.1857	6
3	1	8	0	1.1322	1.1322	7
0	2	8	0	1.1282	1.1281	5
4	0	7	0	1.1244	1.1239	4
2	0	10	0	1.1240	1.1238	4
1	1	10	0	1.1225	1.1224	5
2	2	7	0	1.1188	1.1186	3
5	1	0	0	1.1131	1.1133	1
4	2	0	0	1.1094	1.1094	1
5	1	1	0	1.1086	1.1086	1
1	3	0	0	1.1031	1.1029	2
5	1	2	0	1.0949	1.0951	3
4	2	2	0	1.0918	1.0913	5
1	3	2	0	1.0852	1.0852	3
4	0	8	0	1.0582	1.0581	2
2	2	8	0	1.0536	1.0536	2
5	1	4	0	1.0452	1.0453	3
4	2	4	0	1.0424	1.0421	3
1	3	4	0	1.0367	1.0368	2
2	0	11	0	1.0344	1.0347	3
1	1	11	0	1.0334	1.0337	3
0	0	12	0	1.0130	1.0129	2
5	1	5	0	1.0122	1.0122	2

[a] k_2 is an index for the vector along the b^* axis with a periodicity of q ($= 0.281$) $\times b^*$. a, b, c, and β were calculated from d spacings of hk_1l0. d spacings of hk_1lk_2 were calculated from a, b, c, β, and $q = 0.281$.

diffraction peaks on X-ray powder diffraction patterns of the specimens of both the orthorhombic and monoclinic phases (see Tables 3C and 3D). In these tables are listed the powder data on four-dimensional hk_1lk_2 in which k_2 is an index of the periodicity of $q \times b^*$. The lattice constants of unison-X_1, including q, are listed in Tables 4A and 4B. They are almost independent of the chemical composition of the solid solution; however, q increases with the composition of $In_2Ti_2O_7$ in the both the monoclinic and orthorhombic phases. The relationship between the lattice constant of $a_p = 9.90$ Å of an imaginary "$In_2Ti_2O_7$," which was estimated from Fig. 2, and those of unison-X_1 in the monoclinic or orthorhombic system are approximately as follows:

$$a_m = -\tfrac{1}{4}a_p + (-\tfrac{1}{2})b_p + (-\tfrac{1}{4})c_p,$$

$$b_m = -\tfrac{1}{4}a_p + (0)b_p + (\tfrac{1}{4})c_p,$$

$$c_m = \tfrac{1}{4}a_p + (-\tfrac{1}{2})b_p + (\tfrac{1}{4})c_p,$$

$$\beta(^\circ) = 109.47,$$

$$a_0 = -\tfrac{1}{4}a_p + (-\tfrac{1}{2})b_p + (-\tfrac{1}{4})c_p,$$

$$b_0 = -\tfrac{1}{4}a_p + (0)b_p + (-\tfrac{1}{4})c_p,$$

$$c_0 = \tfrac{2}{3}a_p + (-\tfrac{2}{3})b_p + \tfrac{2}{3}c_p,$$

where $a_p = b_p = c_p = 9.90$ Å.

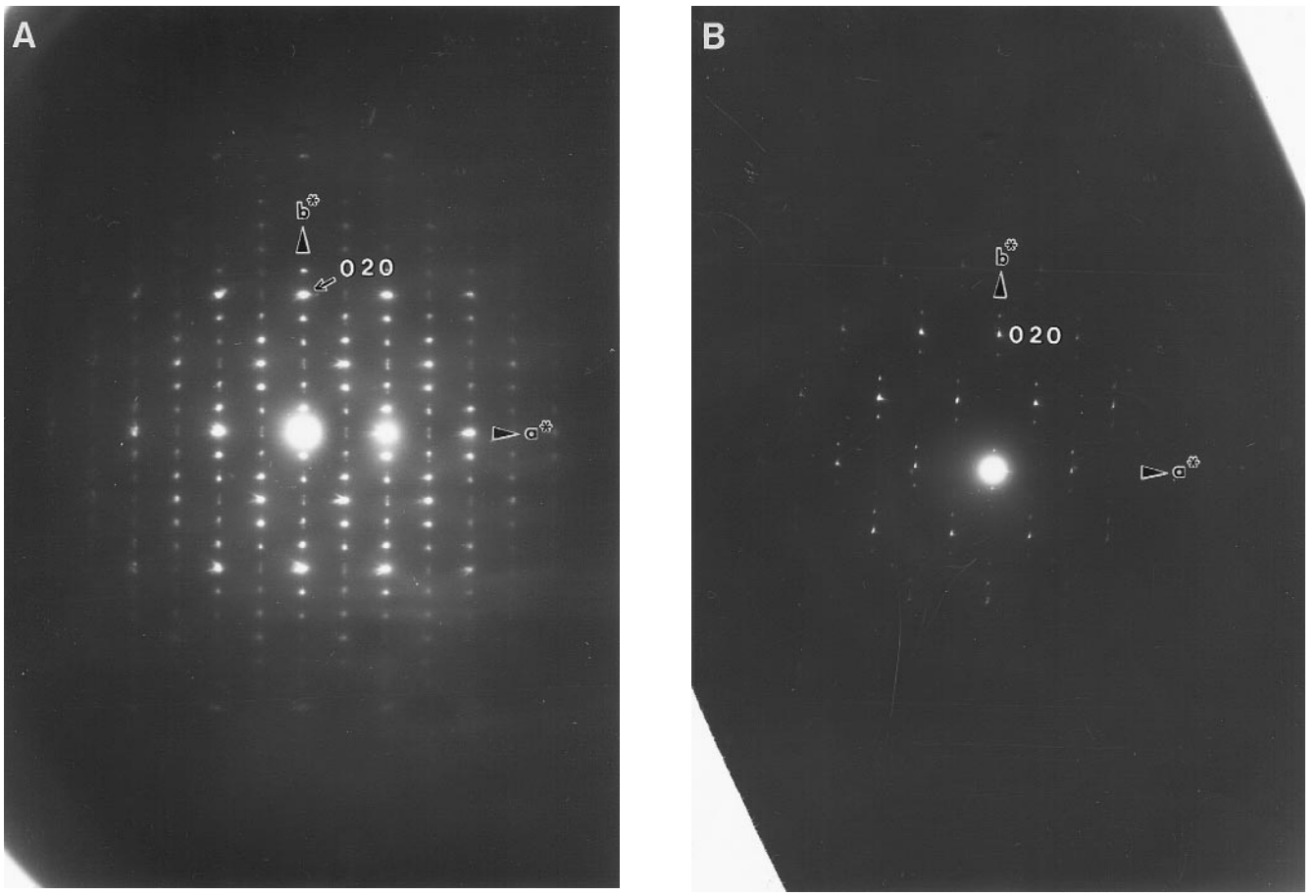

FIG. 3. Electron diffraction photographs of (A) monoclinic $In_3Ti_2FeO_{10}$ and (B) orthorhombic $In_3Ti_2FeO_{10}$.

In Fig. 4, we show the relationship between the unit cell of the cubic pyrochlore and those of the unison-X_1 structures. We conclude that $In_3Ti_2FeO_{10}$ undergoes a phase transformation between 1100 and 1200°C in air. At 1100°C, monoclinic unison-X_1 was formed from In_2O_3, TiO_2, and Fe_2O_3 powders in the full solid solution range, and next, an orthorhombic phase appeared very gradually from the monoclinic phase in the $InFeO_3$-rich region. The monoclinic phase was not fully transformed into the orthorhombic phase in a single phase state at 1100°C because of

TABLE 4A

Lattice Constants and Unit Cell Volumes of Unison-X_1 (Monoclinic System, Extinction Law: $h+k_1 \neq 2n$ for hk_1l0) Prepared at 1100°C[a]

u:*v*:*w*	3:4:1	7:10:2	4:6:1	7:12:1[b]
s:*t*	1:1	4:5	2:3	
a (Å)	5.9171 (5)	5.9165 (6)	5.9158 (6)	5.919 (5)
b (Å)	3.3696 (3)	3.3779 (3)	3.3806 (3)	3.371 (3)
c (Å)	6.3885 (6)	6.3806 (6)	6.3773 (6)	6.378 (5)
β (°)	108.02 (1)	108.04 (1)	108.04 (1)	108.12 (5)
q	0.333	0.350	0.356	
V (Å^3)	121.1	121.3	121.2	120.9

[a]All the specimens have a periodicity with $q \times b^*$ along the b^* axis. *u*:*v*:*w*, mole ratio of In_2O_3:TiO_2:Fe_2O_3; *s*:*t*, mole ratio of $InFeO_3$:$In_2Ti_2O_7$.

[b]There exist three phases: unison-X_1, TiO_2, and In_2TiO_5.

TABLE 4B

Lattice Constants and Unit Cell Volumes of Unison-X_1 (Orthorhombic System, Extinction Law: $h+k_1 \neq 2n$ for hk_1l0 and $k_1 \neq 2n$, $l \neq 2n$ for $0k_1l0$) Prepared at 1200°C for (2+2+3) days[a]

u:*v*:*w*	4:4:2[b]	15:16:7	7:8:3	31:36:13	3:4:1
s:*t*		7:4	3:2	13:9	1:1
a (Å)	5.901 (2)	5.8979 (5)	5.9007 (5)	5.9036 (7)	5.9089 (5)
b (Å)	3.368 (1)	3.3683 (3)	3.3672 (3)	3.3691 (4)	3.3679 (3)
c (Å)	12.146 (4)	12.155 (1)	12.149 (1)	12.148 (1)	12.130 (1)
q		0.281	0.293	0.302	0.3333
V (Å^3)	241.4	241.5	241.4	241.3	241.4

[a]*u*:*v*:*w*, mole ratio of In_2O_3:TiO_2:Fe_2O_3; *s*:*t*, mole ratio of $InFeO_3$:$In_2Ti_2O_7$.

[b]There exist three phases—unison-X_1, Fe_2O_3, and In_2O_3—which were heated at 1100°C.

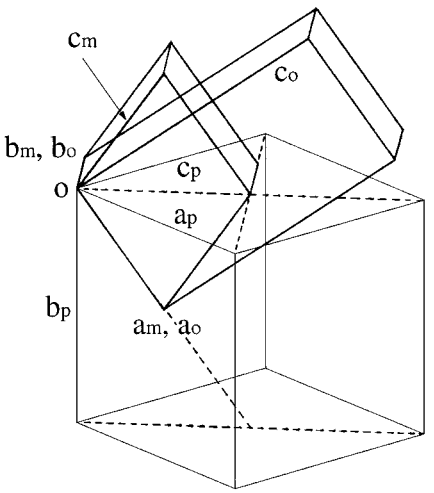

FIG. 4. Relationship between the unit cell of cubic pyrochlore and those of monoclinic and orthorhombic unison-X_1.

the sluggish rate of the phase transformation. Therefore, the limit of the solid solution range of orthorhombic unison-X_1 in the $InFeO_3$-rich region was actually determined from the limit of the unstable monoclinic phase. However, since the reaction rate for the formation of the orthorhombic phase, which is in equilibrium with In_2O_3 and Fe_2O_3, from a mixture of In_2O_3:TiO_2:Fe_2O_3 = 4:4:2 or 4:2:4, for instance, was much faster than that in a single-phase state from the monoclinic phase, we safely conclude that the $InFeO_3$-richer area has the orthorhombic phase.

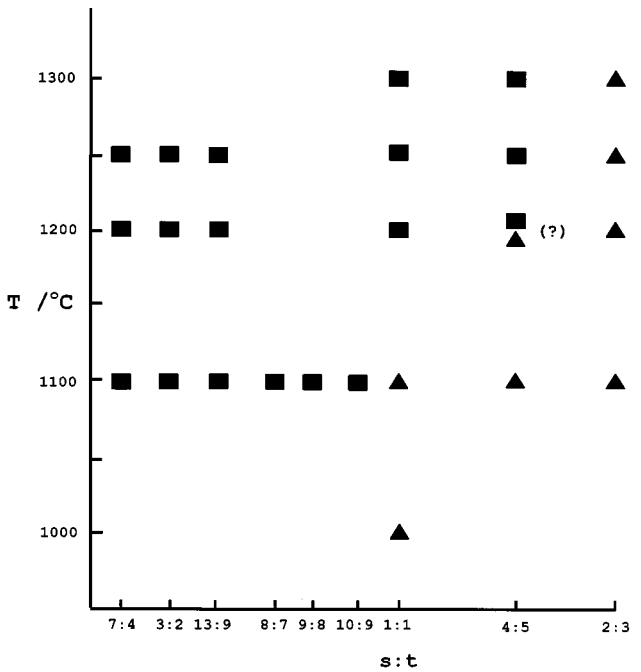

FIG. 5. Dependence of the structure of unison-X_1 on the chemical composition and temperature. s:t, $InFeO_3$:$In_2Ti_2O_7$ mole ratio. ▲, Monoclinic phase. ■, Orthorhombic phase.

In Fig. 5, we show the dependence of the structure of unison-X_1 on chemical composition and temperature. It is clear that the area of the orthorhombic phase expands with higher temperature. At present, although we do not know the detailed crystal structures of the unison-X_1 phases, we conclude that (1) unison-X_1 has a continuous solid solution range along a line between "$InFeO_3$" and "$In_2Ti_2O_7$," (2) it has at least two crystal structures related to the pyrochlore type, (3) $In_3Ti_2FeO_{10}$ has a monoclinic phase at 1100°C and an orthorhombic phase at 1200°C, (4) unison-X_1 has incommensurate diffraction spots along the b^* axis with a periodicity of q ($= 0.281$–$0.356) \times b^*$ in the solid solution range and $q = \frac{1}{3}$ at the chemical composition of In_2O_3:TiO_2:Fe_2O_3 = 3:4:1. We prepared about 30 compounds in the system In_2O_3–TiO_2–A_2O_3–BO (A = A1, Cr, Mn, Fe, or Ga; B = Mg, Mn, Co, Ni, Cu, or Zn) that are isostructural with the monoclinic or orthorhombic phase of unison-X_1. Conditions of synthesis and analysis of their crystal structures including the incommensurate one will be reported soon.

ACKNOWLEDGMENTS

One of the authors (N.K.) expresses his sincere thanks to the late Dr. M. Isobe and Dr. M. Saeki for their helpful discussions and to the Japan International Cooperation Agency for financial support.

REFERENCES

1. R. D. Shannon, *Acta Crystallogr. Sect. A* **32,** 751 (1976).
2. R. D. Shannon, *Solid State Commun.* **4,** 629 (1966).
3. H. R. Hoekstra, *Inorg. Chem.* **5,** 754 (1966).
4. M. Nakamura, N. Kimizuka, and T. Mohri, *J. Solid State Chem.* **86,** 16 (1990).
5. M. Nakamura, N. Kimizuka, and T. Mohri, *J. Solid State Chem.* **93,** 298 (1991).
6. M. Nakamura, N. Kimizuka, T. Mohri, and M. Isobe, *J. Solid State Chem.* **105,** 535 (1993).
7. N. Kimizuka, M. Isobe, T. Mohri, and M. Nakamura, *J. Solid State Chem.* **103,** 394 (1993).
8. N. Kimizuka, M. Isobe, and M. Nakamura, *J. Solid State Chem.* **116,** 170 (1995).
9. N. Kimizuka, E. Takayama-Muromachi, and K. Siratori, *in* "Handbook on the Physics and Chemistry of Rare Earths" (K. A. Gschneidner, Jr. and L. Eyring, Eds.), Vol. 13, Chap. 90, p. 283, North-Holland, Amsterdam, 1990.
10. M. Nakamura and N. Kimizuka, *Jpn. J. Appl. Phys.* **32/33,** Suppl. 184 (1994).
11. J. Senegas, J.-P. Manaud, and J. Galy, *Acta Crystallogr. Sect. B* **31,** 1614 (1975).
12. R. S. Roth, *J. Res. Natl. Bur. Stand.* **56,** 17 (1956).
13. L. H. Brixner, *Inorg. Chem.* **3,** 1065 (1964).
14. M. D. Karkhanavala and A. C. Momin, *J. Am. Ceram. Soc.* **42,** 400 (1959).
15. R. W. Taylor, *Am. Miner.* **49,** 1026 (1964).
16. I. Nodari, A. Alebouyeh, J. F. Brice, R. Gerardin, and O. Evrard, *Mater. Res. Bull.* **23,** 1039 (1988).
17. R. Gerardin, E. H. Aqachmar, A. Alebouyeh, and O. Evrard, *Mater. Res. Bull.* **24,** 1417 (1989).
18. D. M. Giaquinta, W. M. Davis, and H. C. Z. Loye, *Acta Crystallogr. Sect. C* **50,** 5 (1994).
19. R. D. Shannon and C. T. Prewitt, *J. Inorg. Nucl. Chem.* **30,** 1389 (1968).